THE EXTRINSIC THOMSON EFFECT (ETE)

Richard J. Buist

TE Technology, Inc.
1590 Keane Drive
Traverse City, Michigan 49686

There are two well-known thermodynamic effects (with no magnetic field present) that give rise to or enhance the cooling effect in thermoelectric (TE) materials: The Peltier effect and the Thomson effect. The Thomson effect is produced by a Seebeck coefficient gradient induced by the temperature gradient in an operating TE pellet. This paper introduces a third TE cooling effect which is similar to the Thomson effect. It is similar in that it is an "extra" cooling effect brought on by an artificially or extrinsically produced Seebeck gradient. This effect, therefore, shall be referred to as the Extrinsic Thomson Effect (ETE).

Introduction

The principle of the ETE was discovered at the Borg-Warner Research Center, Des Plaines, Illinois, in the early 1960's. It was later patented by Reich [1] in 1971. Technical papers were published on this subject by Reich [2] and Buist [3] in 1972. This effect was experimentally verified over 20 years ago at the Borg-Warner Research Center but was strategically not promoted and went essentially unnoticed in the thermoelectric (TE) industry. Thus, this paper is a re-introduction of the ETE in an effort to advance the future potentials for thermoelectric cooling applications.

Derivation of the ETE

The discovery of the ETE was mathematically based as opposed to laboratory experimentation. It was first derived "on paper" and subsequently verified by experiment. It emerged via analysis of the fundamental one-dimensional thermodynamic equation derived by Domenicali [4]. This equation expressed the thermal equilibrium of a material under an applied electric field.

$$\nabla \bullet (\kappa \nabla T) - T (Je \bullet \nabla S) = -Je^2 \rho \qquad (1)$$

Where:

κ = thermal conductivity,
T = absolute temperature,
Je = current density,
S = Seebeck coefficient, and
ρ = electrical resistivity.

The one-dimensional form reduces to:

$$d/dx (\kappa A dT/dx) - I T dS/dx = -I^2 \rho \qquad (2)$$

Where:

x = dimension in the direction of current flow,
A = cross-sectional area, and
I = current.

The second term of this equation can be expanded as follows:

$$I T dS/dx = I T \delta S/\delta T dT/dx + I T \delta S/\delta x \qquad (3)$$

The first term on the right hand side of equation (3) is the well-known Thomson term:

$$I T \delta S/\delta T dT/dx = \text{Thomson Effect} \qquad (4)$$

The second term in this expression is the ETE term:

$$I T \delta S/\delta x = \text{Extrinsic Thomson Effect} \qquad (5)$$

If the Thomson term is of the proper algebraic sign, it will enhance cooling. Because of the similarity of these terms, if the ETE term is non-zero and of the proper algebraic sign it, too, will enhance cooling. That is, the only difference between these two terms is that in one case the Seebeck coefficient varies intrinsically along the length of the material, while in the other case, the Seebeck coefficient variance is extrinsic.

Model Description

Although rigorous, the equations above are very complicated to solve, given the temperature-dependent nature of TE materials. Therefore, the simple but equally rigorous and accurate TE cooling calculation method presented by Buist [5] was used to carefully examine the nature of the ETE. This modeling process is a numerical method suitable for today's high-speed computational technology available in personal computers. It had been developed to accurately quantify the TE cooling performance in the presence of temperature-produced TE parameter variances in an operating TE pellet. In this case, however, it provided the means for separating the intrinsic versus extrinsic effects produced by parameter variance. As such, it has been employed to clearly and definitively establish the nature and some general principles of the ETE.

An example of the numerical calculation model for a given TE pellet is illustrated in Figure 1. This particular example illustrates how the TE pellet is mathematically dissected into 20 equal-sized segments. Actually, 80 such segments were used in the calculations described herein in order to provide a very high level of resolution and accuracy. The purpose of using multiple segments is allow the use of "constant-parameter" theory which is simple to use and easy to understand.

The calculations proceeded upward from the base, or hot-side, of the TE pellet where the temperature was known. The detailed application of the constant-parameter equations is illustrated in the expanded segment #7, given in Figure 2. Details of this calculation process was given in the paper on this subject by Buist [5]. It had been shown in this paper that this calculation method precisely captures and accounts for the "temperature-induced" Thomson cooling effect and, therefore, would also model the impact of extrinsically induced property gradients. One has only to artificially assign constant values of S, ρ, κ (and, therefore, Z) for each segment and proceed with the calculations as described in the above-referenced paper.

Cold Side

20
19
18
17
16
15
14
13
12
11
10
9
8
7
6
5
4
3
2
1

Hot Side (27°C)

Figure 1: TE Pellet Thermal Model (20 Segments).

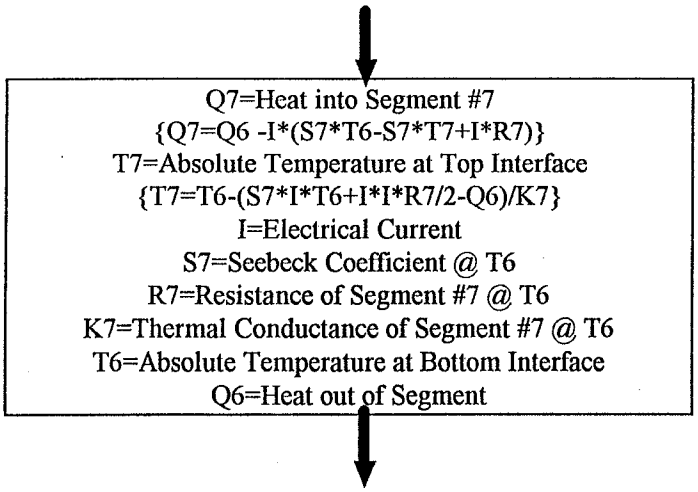

Figure 2: Example Segment #7 description and equations.

Calculations

In order to isolate and illustrate extrinsic effects of TE material parameter variance, each segment of the model was assigned a constant, temperature-independent set of S, ρ, and κ parameters. These data were selected from the set given in table 1. These data were generated subject to the following criteria:

1. All segments of all cases had the same, exact Z.
2. All pellets had approximately the same average S, ρ, and κ.
3. Case 1 was generated by holding S to the average, constant value for all segments and significantly varying ρ and κ from one-half of the pellet to the other. This was done keeping each parameter of each segment within a given half-pellet the same constant value.
4. Case 2 was simply the reverse of case 1.
5. Cases 3, 4, 5 and 6 were similarly generated but sequentially holding ρ or κ constant and significantly changing S from one-half of the TE pellet to the other.
6. Case 7 was generated by holding κ constant, but linearly varying Seebeck for each segment of the pellet.
7. Case 8 was similar to case 7 but with the Seebeck variance in the reverse direction.

Table 1

TE Material Parameters
Used in Calculation Demonstration
($Z=2.7 \times 10^{-3}$ °K^{-1} for all Segments for all cases)

	Description	Seg-ments	Seebeck μV/°C	Rho Ω-m	Kappa W/m/°C
1	Const.S/F	1-40	200	10	1.482
		41-80	200	20	0.741
2	Const.S/R	1-40	200	20	0.741
		41-80	200	10	1.482
3	Const.κ/F	1-40	250	23.15	1.0
		41-80	150	8.33	1.0
4	Const.κ/R	1-40	150	8.33	1.0
		41-80	250	23.15	1.0
5	Const.ρ/F	1-40	250	15	1.543
		41-80	150	15	0.556
6	Const.ρ/R	1-40	150	15	0.556
		41-80	250	15	1.543
7	Special/F	1-80	250-150	15	1.543-0.556
8	Special/R	1-80	150-250	15	0.556-1.543

Mathematical models were constructed for each of the cases indicated in Table 1 and calculations were performed in accordance with the procedures and processes as described above for sequentially selected values of applied current. The results for Cases 1-4 are given in Figure 3. The calculated performance curve for Cases 1 and 2 were totally and exactly the same. In fact, additional calculations performed with various scenarios of changing ρ and κ throughout the pellet had no effect whatsoever on the maximum ΔT as long as S was constant. For these cases, the maximum ΔT was equal to the well-known, constant-parameter expression, $\Delta T_{max} = 1/2\ ZT_c^2$. This is very much what one would expect for constant properties.

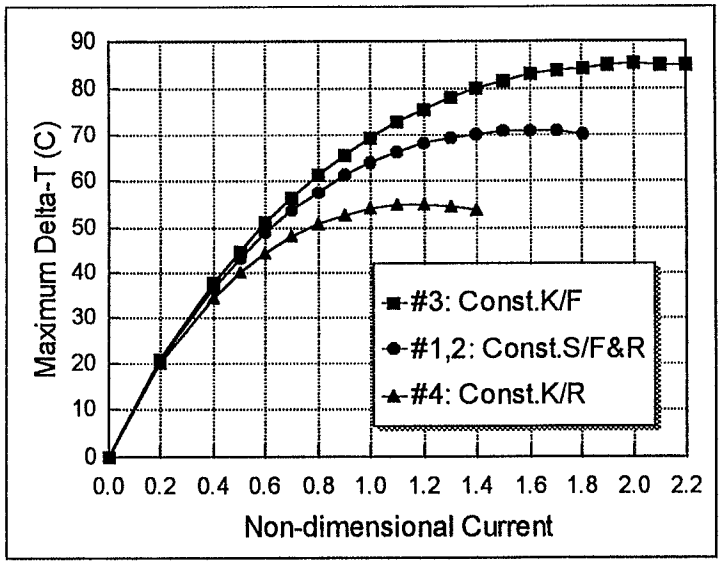

Figure 3: Cooling Performance Calculation for Cases 1-4.

In sharp contrast, the cooling performance curves for variable S were greatly affected as concluded from the equations and analysis given above. Furthermore, the lower ΔTmax for the reverse case was, indeed, consistent with the algebraic sign of

extrinsic Thomson term, equation [5]. These set of curves also illustrate the fact that the forward direction (Case 3) produces its ΔTmax at a current which is higher than what would be predicted from the average properties, while the reverse is true for Case 4.

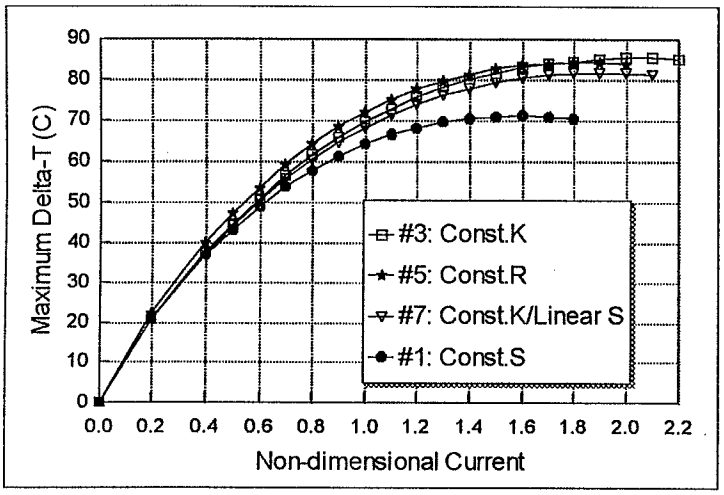

Figure 4: Forward mode performance calculations, cases 1, 3, 5, and 7.

Figure 4 is a similar plot, but for all forward cases studied. There are several interesting effects illustrated in these four cases. One is that there is some observable difference in ΔTmax for when κ is held constant versus holding ρ constant even with exactly the same S variance. Thus, there appears to be some secondary interactive, but minor impact of ρ and κ variance, not at all evident whenever S is held constant. The more dramatic observation is the lower ΔTmax for the case where S is varied linearly versus the step-function mid-way along the pellet.

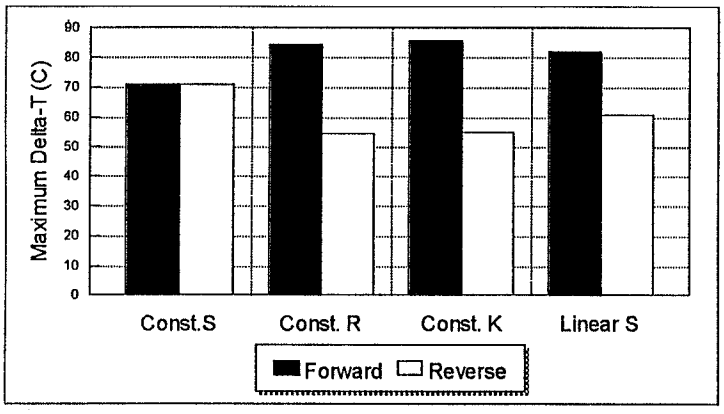

Figure 5: ΔTmax calculations for all cases studied.

The ΔTmax results for all 8 cases studied are summarized in Figure 5. Clearly, this is dramatic evidence of the ETE, ruling out the possibility that the observed enhancements may have been caused by the naturally less Joule heat produced in the cold half of the TE pellet where ρ is low when S is low.

Test Data

There was one very convenient result observed from these study cases: There was no apparent penalty, and perhaps it was even desirable, to produce ETE enhancement with an abrupt, step-functional variance in Seebeck coefficient. This allowed for the fabrication of simple, but effective, ETE devices by soldering TE pellet segments together as shown in Figure 6. Alternatively, powder metallurgy can totally eliminate the extra solder interface.

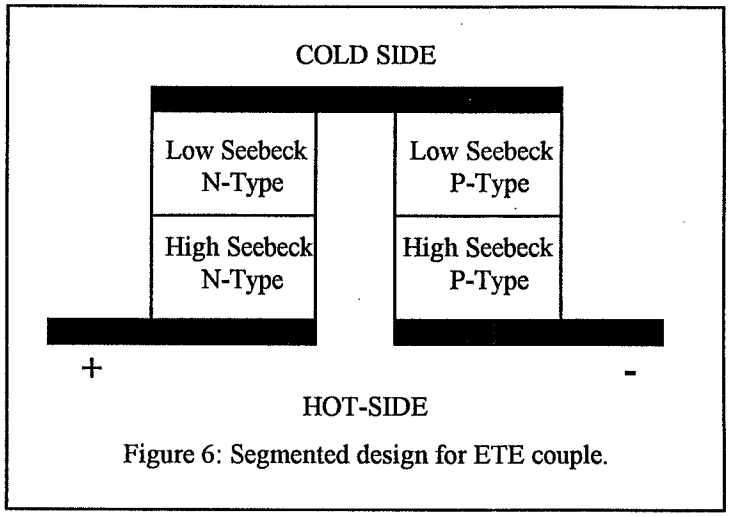

Figure 6: Segmented design for ETE couple.

Single test couples such as that illustrated in Figure 6 were fabricated by simply soldering high and low Seebeck, N and P-type segments together. This work was performed during the late 1960's by the author at the facilities at the Borg-Warner Research Center in Des Plaines, Illinois. Also, High-S and Low-S control couples were fabricated from homogeneous pellets extracted from the same TE material wafers as those used to form the segments of the ETE couple. All couples were then instrumented with thermocouples and all mounted together on the same, temperature controlled base plate within a vacuum system. The base plate was held to 27°C for all test points. The vacuum was held to approximately $5x10^{-5}$ Torr. The test configuration was a large bell jar with no radiation shielding employed whatsoever. The applied current was stepped sequentially and held constant to allow for steady-state testing. The results are shown in Figure 7. Clearly, these tests validated the existence of the ETE as a new, additive TE cooling effect with performance enhancement far above that produced via intrinsic means.

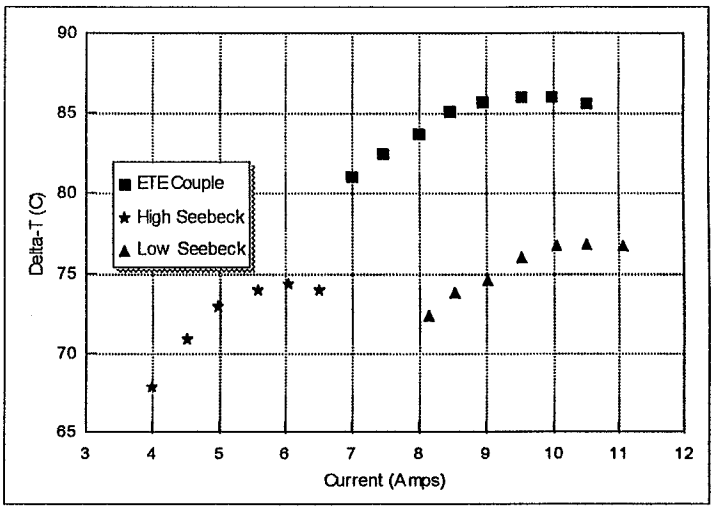

Figure 7: Test data on a 2-segment ETE couple versus homogeneous couples fabricated from low and high S TE materials from which the ETE couple was produced.

As one might surmise, the ETE is increased for larger and larger Seebeck gradients. However, the penalty for that is lower and lower average Z. That is, there will be some Seebeck value for TE cooling material for which Z is maximized. As Seebeck is varied left and right of this maximum, Z falls off, thereby sacrificing the primary cooling effect. It is nevertheless true that

the ETE is so large that is produces significant overall cooling enhancement even though the average Z is sacrificed.

In order to further enhance cooling performance, a three-segment TE pellet was produced and tested at Borg-Warner Research Center by inserting a medium Seebeck, high Z segment in the middle, as shown schematically in Figure 8. The measured values of Seebeck and Z for each segment were as shown.

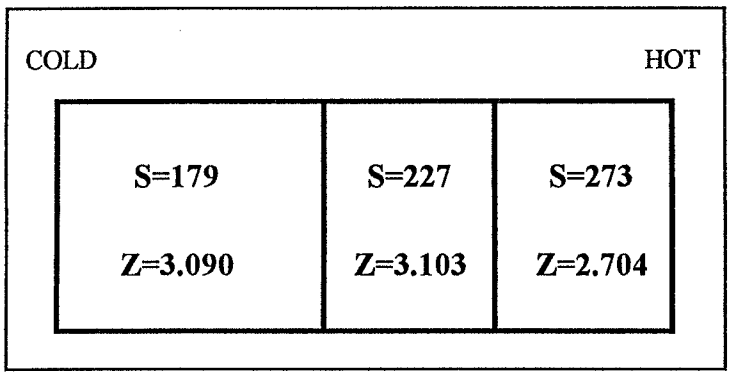

Figure 8: Schematic for 3-segment ETE test pellet.

This was a single, N-type TE pellet and was tested as such in a vacuum system using a special test fixture. It provided a pre-cooled electrical connection at a temperature always slightly above the cold junction of the test pellet. As such, the cold electrode was assured to always apply a slight heat load to the test pellet in order to preclude the possibility for external cooling of the test pellet.

The test results of this 3-segment TE pellet are given in Figure 9. This produced a dramatic maximum ΔT of 92.5°C from a 27°C hot side temperature and set the standard for a whole new state-of-the-art in single-stage TE cooling devices.

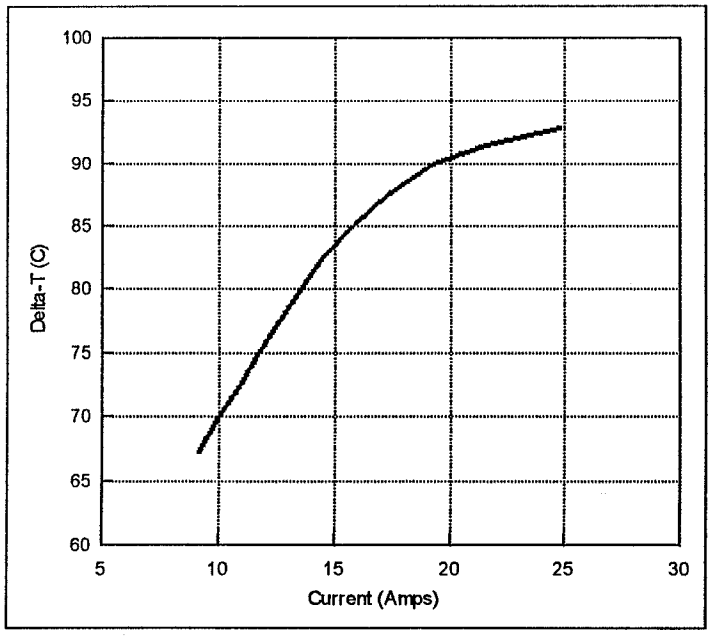

Figure 9: Test data on 3-segment ETE pellet.

Conclusions

The Extrinsic Thomson Effect was initially discovered on paper by simply not ignoring one of the terms that resulted from the fundamental heat balance equation. Like many good discoveries, it seems simple and obvious once disclosed. Nevertheless, it has gone unnoticed and un-exploited since its discovery more than 35 years ago.

The Thomson effect was known to enhance TE cooling because of the positive dS/dT slope of typical TE cooling materials near room temperature. Thus, it was surmised that if a TE pellet were produced with an artificially produced extrinsic Seebeck variance in the same direction, it also would enhance TE cooling.

Initial experiments proved this to be the case and inhomogeneous TE pellets and couples were produced which significantly out-performance any homogeneous TE couple even today, 35 years later.

Now, with the precision of numerical models and high-speed computers, demonstrations have clearly re-established the nature of the ETE phenomenon and have provided the means for practical device design optimization. It is hoped that the ETE can be exploited by all thermoelectricians to set new standards for thermoelectric cooling for the challenging years that face our industry.

References

[1] A.D. Reich, M. Stanley and K. Kountz, U.S. Patent Number 3,564,860 (1971).

[2] A.D. Reich, Infrared Information Symposium (IRIS) meeting proceedings (1972).

[3] R.J. Buist, Infrared Information Symposium (IRIS) meeting proceedings (1972).

[4] C.A. Domenicali, "Irreversible Thermodynamics of Thermoelectricity", Reviews of Modern Physics, vol. 26, pp.237-275, (1954).

[5] R.J. Buist, "Design and Engineering of Thermoelectric Cooling Devices", 10th International Conference on Thermoelectrics, Cardiff, Wales, September 10-12, (1991).